34th Annual International Conference of the IEEE EMBS
San Diego, California USA, 28 August - 1 September, 2012

Development of Gait Segmentation Methods for Wearable Foot Pressure Sensors

S. Crea, S. M. M. De Rossi, M. Donati, P. Reberšek, D. Novak, N. Vitiello, T. Lenzi, J. Podobnik, M. Munih, M. C. Carrozza

Abstract— **We present an automated segmentation method based on the analysis of plantar pressure signals recorded from two synchronized wireless foot insoles. Given the strict limits on computational power and power consumption typical of wearable electronic components, our aim is to investigate the capability of a Hidden Markov Model machine-learning method, to detect gait phases with different levels of complexity in the processing of the wearable pressure sensors signals. Therefore three different datasets are developed: raw voltage values, calibrated sensor signals and a calibrated estimation of total ground reaction force and position of the plantar center of pressure. The method is tested on a pool of 5 healthy subjects, through a leave-one-out cross validation. The results show high classification performances achieved using estimated biomechanical variables, being on average the 96%. Calibrated signals and raw voltage values show higher delays and dispersions in phase transition detection, suggesting a lower reliability for online applications.**

I. Introduction

The detection of gait phases is a critical component of gait analysis, and is fundamental in a variety of fields, including clinical gait analysis and biomechanics [1]. Gait-phase related signals have been also proposed and applied as control variables for functional electrical stimulation and for active robotic prosthesis. In all these application fields, the development of automated and reliable methods to replace the human expert in performing the analysis of gait signals is of clear advantage. Automated gait segmentation methods [2][3][4] have been found particularly interesting in combination with the use of wearable sensors, with the advantage of bringing gait analysis outside the laboratory environment and allowing to perform all-day-long measurements. Wearable sensors to measure foot plantar pressure [4] are a natural choice to perform gait segmentation, since they provide critical measurements related with gait phases.

In this work, we propose an automated segmentation method based on the analysis of plantar pressure signals recorded from two synchronized wireless foot insoles [5], using a common machine-learning technique, Hidden Markov Models (HMMs, [6]). Given the strict limits on computational power and power consumption typical of wearable electronic components, in this work we focus on the development of a (computationally) simple method with high segmentation performances, starting from a previous method presented in [7]. In particular, our aim is to investigate the capability of a HMM machine-learning method to detect gait phases with different levels of complexity in the pre-processing of the wearable pressure sensors signals. We try to evaluate the best compromise between trying to keep a low computational cost, and the need of a high segmentation reliability and precision.

Manuscript received March 15, 2012. This work was supported in part by the EU within the EVRYON Collaborative Project STREP (FP7-ICT-2007-3-231451) and by the CYBERLEGs Project (FP7-ICT-2013-287894). S. Crea, S.M.M. De Rossi, M. Donati, N. Vitiello, T. Lenzi and M.C. Carrozza are with The BioRobotics Institute, Scuola Superiore Sant'Anna, viale Rinaldo Piaggio 34, Pontedera (PI), Italy. (S.Crea is corresponding author, phone: +39 3395604441; e-mail: s.crea@sssup.it).

P. Rebersek, D. Novak, J. Podobnik and M. Munih are with the Laboratory of Robotics, University of Ljubljana, Slovenia.

II. Methods

A. Subjects and Protocol

Five healthy young subjects (age: 28.8 ± 3.6) were chosen to span a wide range of body mass (weight 60-82 Kg, average 72.6 ± 9.0, height 173.2 ± 2.2 cm), with a similar shoe size (41.5-43 EU size). Subjects wearing athletic shoes, equipped with an in-shoe pressure measurement system [5] (see Figure 1) were asked to walk on a straight line at normal pace speed which was chosen freely by each subject. 150 steady-state steps were recorded for each subject, 750 steps in total. Transitory steps (initial and terminal steps) were not processed. The main characteristics of the subjects are summarized in Table I.

B. Measurements System

Two pressure-sensitive insoles were inserted in the shoes of the subject, in place of the regular ones. This device, presented in [5], is made of an array of 64 optoelectronic pressure sensors embedded in a layer of silicone. The sensor technology was presented in [8][9]. The wearable sensor array measures the pressure over the plantar area and transmits the data sampled at a 100Hz frequency, wirelessly to a remote data logging computer.

C. Data Processing and Dataset Building

For each foot, the 64 voltage signals are converted into their relative force values though a non-linear pre-computed function. Pressure values are then extracted through a calibration function (see [5]) and a Laplacian surface

TABLE I
SUBJECT CHARACTERISTICS

Subject	Age [y]	Weight [Kg]	Height [cm]	Shoe Size [EU size]
1	34	60	176	41.5
2	25	82	172	42
3	31	80	171	41.5
4	27	68	175	43
5	27	73	172	42

978-1-4577-1787-1/12/$26.00 ©2012 IEEE

Figure 1. Pressure sensitive insole used in the experiment. In black, the array of pressure sensors covered by a silicone layer. In white, the housing for the electronics. Picture from [5].

smoothing algorithm is applied to the pressure map to remove pressure outliers and regularize the surface. The pressure map is used to extract the values of vertical ground reaction force (vGRF) and the position of the center of plantar pressures (CoPX, CoPY).

According to the different level of pre-processing complexity, three input datasets are built:

- Raw Signals: it includes the first 8 principal components of the 128 (64 for each foot) raw voltage signals recorded at each instant;
- Calibrated Signals: it includes the first 8 principal components of the 128 calibrated pressure values;
- Biomechanical Variables: this dataset is made of 8 biomechanical variables, 4 for each foot: vGRF and CoPY and their first-order-time derivatives. These variables are classically employed to divide the gait into phases [1].

D. Gait Segmentation

The gait model used in this work divides the gait into six phases, according to a simplified version of the classic gait model by Perry [1]. The right foot was taken as reference for the segmentation. Gait phases are defined as follows:

- *LR*: Loading Response. It begins with right floor contact and continues until the left foot is lifted for swing.
- *MS*: Mid Stance. It begins as the left foot is lifted and continues until body weight is aligned over the right forefoot. This phase is connected to the upward acceleration of the body, which unloads the supporting foot.
- *TS*: Terminal Stance. It begins with right heel rise and continues until left foot strikes the ground. This phase concludes the right stance (and left swing).
- *PS*: Pre-Swing. It begins with initial contact of the left limb and ends with the right toe-off. The right limb uses its freedom to prepare for the rapid demands of swing.
- S_1: Swing (1). This phase starts from the end of *PS* and ends when the left vGRF reaches its low peak.
- S_2 : Swing (2). This phase is comprised between the left low peak and the right-foot heel strike.

The gait model employed in this work is a simplified version of classic Perry's model [1], which divides each cycle into 8 phases. Our simplified version does not include the so-called Initial Contact, occurring when the right foot just touches the floor, because it is identified by a rapid peak that cannot be captured with the working bandwidth. Our model is also less specific in the segmentation of the swing phase.

The whole dataset was manually segmented by an expert who analyzed ground reaction force profiles, and marked the transitory events dividing each cycle into the six phases. An example of segmentation is shown in Figure 2.

E. Machine Learning

We hypothesize that the observed signals are modeled by a 6-states Hidden Markov Model (HMM) [6], with 8 observable states (emissions). Let $S=\{S_i,i=1..6\}$ be the set of hidden states, corresponding to the set {*LR, MS, TS, PS, S_1, S_2*}, and $Z=\{z_1,..,z_8\}$ the set of observable emissions.

We chose a left-right cyclic model, which represents well the gait phase pattern during steady-state conditions.

The underlying Markov Model is defined by a set of parameters $\lambda=(\pi,A,B)$, where

$$\pi_i = \Pr[X(t_0)=S_i, i=1,..,6]$$

is the prior probability vector (probability of the Markov chain to occupy a certain state at t_0), A is the 6x6 state transition probability matrix, defined by

$$\begin{cases} A_{ij} = \Pr\left[X(t_{n+1}) = S_j \mid X(t_n) = S_i\right] \\ \sum_{i=1}^{6} A_{ij} = 1, \forall j \end{cases}$$

and B is the 8x6 emission matrix, which describes, for each state, a univariate Gaussian random variable of the emissions. In particular,

$$B_{ij}=(\mu_{ij},\sigma_j)$$

where the contribution of the state j to the emission z_i is a random variable $N(\mu_{ij},\sigma_j)$. Following our choice of a left-right model, the only allowed transitions ($A_{ij}>0$) are those to the same state A_{ij} and to the subsequent state A_{ij+1}.

Starting from the segmentation performed by the expert, each observed emission at time t was labeled with a reference state $S_{ref}(t)$. The reference labeling was used partly to train the HMM, and partly to evaluate the performances of the automated segmentation method.

The Leave-One-Out Cross-Subject Validation (LOOCV) approach was applied to the training and validation of the method. In particular, the union of data gathered from N=Q-1=4 subjects (600 gait cycles) was used to train and optimize the HMM, while data from the remaining subject (150 gait cycles) was used for validation. LOOCV was applied five times to all possible subject subsets to test the generalization capabilities of the method.

The model parameters λ were estimated from the training dataset through a simple statistical estimation method. The transition matrix elements A_{ij} were calculated as

$$A_{ij} = \frac{T_{ij}}{N_i}$$

where T_{ij} is the number of samples of the training dataset with a transition from state S_i to state S_j, and N_i is the total number of samples labeled with state S_i. The elements of emission matrix B were computed by respectively the sample mean and sample standard deviation of the emissions in each state. The prior probability vector was set to π= (1,0,0,0,0,0) to represent the known state *LR* from which all observations started. Testing of the method was done using the Viterbi decoding algorithm, which estimates the most likely state $S_{est}(t)$ based on the previous estimation $S_{est}(t-1)$ and current observable emissions Z(t). The Viterbi algorithm was run on

the entire testing dataset, and the estimated labeling was then compared to the reference to evaluate its performances.

A common problem when using the Viterbi algorithm in left-right HMMs is that of *deletions* and *insertions* [6], consisting respectively in missed detections of full gait cycles, and erroneous insertion of quick cycles. A solution to the problem of insertions is that of imposing a minimal duration to each state S_i, in which transitions decoded before the minimum phase length are rejected.

Implementation of the HMMs and of the Viterbi decoding algorithms were done using MATLAB® by Mathworks, and the HMM toolbox [10].

F. Evaluation of Performances

The performance of the algorithm was evaluated with the LOOCV method based on two indices. On one side, we computed the percentage of right classifications n, as

$$n = \frac{\#(S_{est}(t) = S_{ref}(t))}{\#S_{ref}(t)}$$

The performance n was computed over the whole dataset, outside of a tolerance window of 5 samples (50ms) about each reference transition. The tolerance window accounts for a minimal discretionary variability in the estimate, which is also present in the segmentation by the expert. The precision of the method was also evaluated by computing the average and standard deviation of delays of the detected transitions.

III. Results

Table II reports the classification performances of the automated algorithm in terms of percentage of correct (and wrong) estimates. Results are shown for the three different datasets. Each row of the table corresponds to the HMM being trained on the dataset from 4 out of 5 subjects, and tested on the remaining subject. In the last row the classification average across all subjects is reported.

Table III shows separately for each dataset the average and standard deviation of the delays in terms of number of samples, for each phase transition. Delays are calculated as the difference between the moment of the estimated and the reference transition. The last column of the tables shows a total performance index across subjects, calculated as the root mean square of the average delays and the average of standard deviations for each phase transition. This index summarizes the dispersion of the delays around the mean value for each transition.

IV. Discussion

The overall performance shown by our method in Table II denotes a high specificity in the capacity to segment and classify the gait cycle into sub-phases when biomechanical variables are used. The average performance of 95.9% right classification (94.9%-96.8%) corresponds roughly to 6 wrong samples for each gait cycle, for an average of 1 for each phase transition. This performances are in line with state-of-the-art methods [2][3][4]. Performances markedly fall when the simple raw or calibrated signals are used, despite the second dataset (72.3%-88.4%) exhibits better performances if compared with the first one (70.7%-80.3%). The highest performances reached with the biomechanical

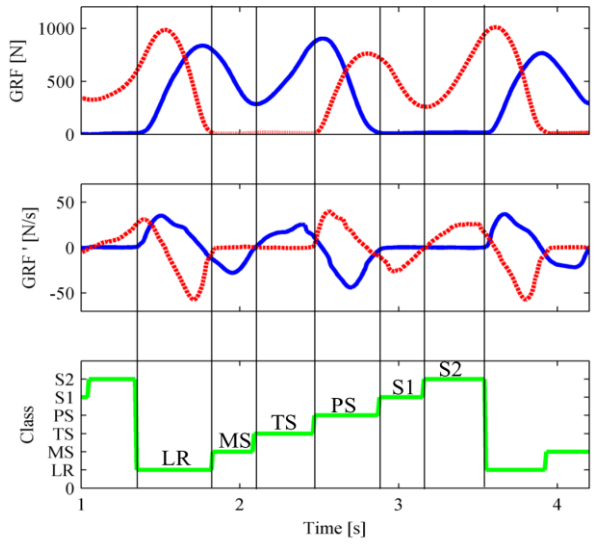

Figure 2. Example of segmentation of a gait cycle in sub-phases made by the expert. On the two top panels, vertical ground reaction forces from the right (solid line) and left (dashed line) insoles, and their first-order-time derivatives. On the bottom panel, the reference segmentation is shown, with transitions highlighted by vertical lines.

variables dataset can be explained by two reasons: on one side, the reference segmentation was performed on the total ground reaction force profile; on the other side, aggregated variables are less noisy then raw variables given the complex smoothing techniques used to extract them. Moreover, the use of raw signals showed the further disadvantage of *deletions* which do not occur when calibrated values or biomechanical variables are used.

The Total Index showed in Table III demonstrates the high capability of the algorithm to detect phase transition when biomechanical variables are used. *Phase3-Phase4* transition and the 'twin' *Phase6-Phase1* transition are recognized by the model with high precision, having the lowest average delays and low standard deviations (0.8±3.7 for *Phase3-Phase4*, 1.3±1.7 for *Phase6-Phase1*). The worst cases in terms of average delay and dispersion are *Phase2-Phase3* and *Phase5-Phase6* transitions. This behavior is probably due to the less pronounced landmarks in the curves, which generates a higher variability in phase transition detection when manual segmentation is carried on and, consequently, when testing is performed. Also calibrated and uncalibrated signals datasets exhibit the highest variability within transition from *Phase5* to *Phase6*. They show, however, higher dispersions even in all the other phase transitions, suggesting a lower reliability in online applications. A

TABLE II
PERCENTAGE OF RIGHT (WRONG) CLASSIFICATION IN THE TESTING SET

	Raw [%]	*Calibrated [%]*	*Biomechanical Variables [%]*
Subject 1	80.3(19.7)	88.4(11.6)	96.3(3.7)
Subject 2	71.6(28.4)	81.9(18.1)	95.9(4.1)
Subject 3	71.6(28.4)	72.3(27.7)	96.8(3.2)
Subject 4	79.9(20.1)	78.1(21.9)	94.9(5.1)
Subject 5	70.7(29.3)	78.8(21.2)	95.5(4.5)
Average	*74.8(25.2)*	*79.9(20.1)*	*95.9(4.1)*

TABLE III
AVERAGE AND STANDARD DEVIATION OF DELAYS IN TERMS OF NUMBER OF SAMPLES FOR PHASE TRANSITIONS IN THE TESTING SET

Raw Signals

	Subject 1	*Subject 2*	*Subject 3*	*Subject 4*	*Subject 5*	*Total Index*
Phase1-Phase2	12.6±6.2	-4.8±11.6	4.3±11.5	5.3±4.9	6.9±10.6	7.4±9.0
Phase2-Phase3	4.0±6.6	8.8±11.0	7.6±10.9	4.6±6.1	6.4±12.9	6.5±9.5
Phase3-Phase4	-7.4±4.1	8.4±12.2	17.3±13.5	-6.5±6.5	-2.9±8.9	9.7±9.0
Phase4-Phase5	-1.9±8.6	3.0±15.6	-0.2±8.9	6.6±9.3	4.2±5.2	3.8±9.5
Phase5-Phase6	-3.1±10.6	15.1±11.9	-7.9±14.6	2.4±12.1	4.7±9.7	8.1±11.8
Phase6-Phase1	-1.5±5.6	12.2±18.9	-0.4±10.7	-7.8±13.8	2.3±5.8	6.6±11.0

Calibrated Signals

	Subject 1	*Subject 2*	*Subject 3*	*Subject 4*	*Subject 5*	*Total Index*
Phase1-Phase2	-2.0±5.9	-0.6±5.8	3.8±7.7	8.5±6.0	1.4±9.6	4.3±7
Phase2-Phase3	-6.6±6.3	2.9±8.5	8.2±8.1	4.3±9.5	12.3±12.1	7.6±8.9
Phase3-Phase4	-4.2±1.8	8.0±10.2	11.5±11.7	3.0±8.3	1.2±10.5	6.7±8.5
Phase4-Phase5	2.9±3.7	2.1±7.1	7.8±7.1	10.7±12.1	5.0±2.9	6.5±6.6
Phase5-Phase6	0.7±8.6	8.2±11.3	9.9±9.7	1.9±13.2	0.1±12.3	5.8±11.0
Phase6-Phase1	-6.3±4.3	10.4±5.1	18.5±16.5	-8.0±5.9	9.4±11.1	11.3±8.6

Biomechanical Variables

	Subject 1	*Subject 2*	*Subject 3*	*Subject 4*	*Subject 5*	*Total Index*
Phase1-Phase2	1.6±2.7	0.2±1.4	0.9±2.0	2.4±2.4	-3.8±4.2	2.2±2.5
Phase2-Phase3	2.1±4.0	3.7±6.4	1.2±3.6	2.3±4.6	4.4±4.3	3.0±4.6
Phase3-Phase4	-1.0±4.2	-1.1±3.6	0.6±4.3	-0.8±2.3	-0.2±3.9	0.8±3.7
Phase4-Phase5	3.3±2.9	0.9±4.2	1.7±3.9	4.6±3.6	0.2±1.1	2.7±3.1
Phase5-Phase6	5.2±5.5	5.9±12.2	4.5±7.4	6.9±7.0	4.0±4.7	5.4±7.4
Phase6-Phase1	-1.2±1.3	-1.1±1.1	-1.0±0.8	-1.6±1.5	1.7±3.7	1.3±1.7

comparison between raw and calibrated signals suggests that the average delays are lower for calibrated dataset for transitions *Phase1-Phase2 Phase3-Phase4* and *Phase5-Phase6*, while in the other cases raw dataset exhibits better results. Despite this, dispersion around the average delays, quantified by the average standard deviation, is lower for all transitions, with the calibrated dataset. This suggests that the calibrated signal set allows for a higher reliability and consistency in the estimation of phase transitions.

V. CONCLUSION

We presented an automated gait segmentation method based on HMM applied to signals coming from a set of wearable foot insoles. The HMM was trained and tested on three types of input, differing for the complexity of the pre-processing applied to raw pressure signals.

The highest performances are reached with dataset formed by the biomechanical variables, which require an expensive calibration to be performed (94.9%-96.8%). Performances achieved using the calibrated dataset are between 72.3% and 88.4%, while those reached using raw voltages range between 70.7% and 80.3%. This suggests that it is extremely difficult to reach high (>90%) specificity values if only simple data processing methods are used.

Future works will be focused on decreasing the computational cost required to compute the biomechanical variables, to reduce average and dispersion of delays and make the algorithm reliable in the detection of gait initiation and termination.

VI. REFERENCES

[1] J. Perry. *Gait Analysis: Normal and Pathological Function*. *Journal of Pediatric Orthopaedics*. Vol. 12. Slack Incorporated, 1992.

[2] A. Mannini, A. M. Sabatini. "A hidden Markov model-based technique for gait segmentation using a foot-mounted gyroscope." In *2011 Annual International Conference of the IEEE Engineering in Medicine and Biology Society*, 4369-4373.

[3] A. Miller. "Gait event detection using a multilayer neural network." *Gait & posture* 29, no. 4 (June 2009): 542-5.

[4] K. Kong, M. Tomizuka. "Smooth and continuous human gait phase detection based on foot pressure patterns." *2008 IEEE International Conference on Robotics and Automation* (May 2008): 3678-3683.

[5] S. M. M. De Rossi, T. Lenzi, N. Vitiello, M. Donati, A. Persichetti, F. Giovacchini, F. Vecchi, and M. C. Carrozza. "Development of an in-shoe pressure-sensitive device for gait analysis." In *Engineering in Medicine and Biology Society (EMBC), 2011 Annual International Conference of the IEEE*, 5637-5640, 2011.

[6] P. A. Devijver, J. Kittler. *Pattern recognition: A statistical approach*. Prentice/Hall International, 1982.

[7] S. M. M. De Rossi, S. Crea, M. Donati, P. Reberšek, D. Novak, N. Vitiello, T. Lenzi, J. Podobnik, M. Munih, M. C. Carrozza, "Gait Segmentation Using Bipedal Foot Pressure Patterns", *IEEE International Conference on Biomedical Robotics and Biomechatronics*, June 24-28, 2012 Roma, Italy.

[8] S. M. M. De Rossi, N. Vitiello, T. Lenzi, R. Ronsse, B. Koopman, A. Persichetti, F. Vecchi, A. J. Ijspeert, H. van der Kooij, and M. C. Carrozza. "Sensing Pressure Distribution on a Lower-Limb Exoskeleton Physical Human-Machine Interface." *Sensors* 11, no. 1 (2010): 207–227.

[9] T. Lenzi, N. Vitiello, S. M. M. De Rossi, A. Persichetti, F. Giovacchini, S. Roccella, F. Vecchi, and M. C. Carrozza. "Measuring human–robot interaction on wearable robots: A distributed approach." *Mechatronics* 21 (2011): 1123-1131.

[10] K. Murphy. Hidden Markov Model (HMM) Toolbox for Matlab (1998).